Available online www.jocpr.com

Journal of Chemical and Pharmaceutical Research, 2013, 5(6):43-49

Research Article

ISSN : 0975-7384
CODEN(USA) : JCPRC5

Computational fluid dynamics analyzing to optimize tangential-inlet swirl nozzle for preparing nano-drug during a SEDS process

Kefeng Xiao[1,2] and Zhihui Hao*[1]

[1]Laboratory of Bio-pharmacy of Agricultural, College of Chemistry and Pharmacy, Qingdao Agricultural University, Qingdao, China
[2]School of Mechanical Engineering, Shandong University, Jinan, China

---

ABSTRACT

A tangential-inlet swirl nozzle for preparing nano-drug during a solution-enhanced dispersion by supercritical CO_2 (SEDS) process has been designed to enhance mixing in a micro-mixing volume. The structure and dimensions of the nozzle are presented. A three-dimensional simulation by using computational fluid dynamics (CFD) and heat transfer during a SEDS process has been performed. The solver used was a commercial code, Fluent 6.3. The length of the swirl chamber and the outlet diameter of the nozzle were chosen as the main factors to be analyzed and optimized. Volume fraction of ethanol and turbulence intensity of mixture were the main indicators to optimize the structure of the nozzle. Results indicated that when the length of swirl chamber was 6mm and the outlet diameter was 0.3mm, supercritical CO_2 and ethanol can mix thoroughly, and the turbulence intensity was high enough to ensure full precipitation of the solute and reduce the time of nucleation growth. The method of CFD analysis used in this work can also be applied to similar systems and can help to improve the performance of the SEDS micronization apparatuses.

Keywords: tangential-inlet swirl nozzle; CFD analysis; SEDS process; nano-drug;

INTRODUCTION

Nano-drug prepared with a controlled particle size and size distribution has many applications in the field of pharmaceutical drug delivery, controlled release, and needleless powder injections[1-3]. Crystallization by supercritical fluid technology (CSFT) has been utilized more and more widely in preparing nano-drug. CSFT is categorized into two types: supercritical anti-solvent (SAS) and rapid expansion of supercritical solution (RESS). In both of the two processes, drug solution generates oversaturation in SCF so as to prepare nano-drug. However, the mechanisms of the two processes are different. In terms of RESS process, drug candidate should have high solubility in supercritical CO_2, and then sprays, crystallizes. However, many drugs cannot be dissolved in SC-CO_2, which limit the use of RESS. In SAS process, what the drug candidate should meet is that it can be dissolved in certain kind of organic solvent. When the solution is introduced into nozzle to mix with SC-CO_2, the solubility of solute reduces quickly. Then, the solute precipitates because of supersaturation and then spray out promptly forming nano-drug. Solution enhanced dispersion by supercritical fluid (SEDS) has been developed based on the principle of SAS. Jet breakup in the spray process has been suggested a controlling factor in SCF anti-solvent precipitation[4]. Consequently, nozzle is core component in SEDS process. It should effectively atomize the solution of active substance(s) in SCF and intensify the mixing of the SCF[5, 6] and the active substance solution for increased transfer rates in order to obtain ultrafine particles with a narrow size distribution by SEDS process[7]. Many nozzle have been designed for SEDS process by researchers, such as jet-swirl nozzle [8], coaxial nozzles[9] and prefilming atomizer[7]. Yet these mixing configurations fail to solve these problems such as an unexpected deposition on the inner wall, frequent agglomeration, inadequate mixing within the nozzle. Computational Fluid Dynamics (CFD) has been an important method to simulate the complex flow[10, 11]. In this paper, a tangential-inlet swirl nozzle for preparing nano-drug by SEDS process was designed and optimized by CFD simulation with the aim of evaluating the turbulence in the nozzle, reducing agglomeration and studying specific situation of these two phrases mixing and turbulence intensity within the nozzle.

STRUCTURAL DESIGN OF NOZZLE

The nozzle that utilizes a swirling flow to optimize mixing between the solution and antisolvent in a micro-mixing volume is designed especially for the SEDS process. The sketch of the structure can be shown in Figure 1. The main feature of this nozzle design is that solution and anti-solvent are injected respectively from two tangential inlets and mixing of the jets occurs within the swirl chamber of the nozzle.

Compared with axial fluid injection, fluid injection from tangent direction of the swirl chamber can reduce momentum loss and enhance tangential speed. The application of swirl flow plays the role of enhancing mixing because swirl flow produce strong shear stress, high turbulence, and rapid mixing rates. The swirling liquids with a high centrifugal force will disrupt into individual droplets when not confined. The centrifugal force is imparted to the bulk liquid by a free vortex in the swirl chamber. The swirling liquid in the swirl chamber produce a swirling hollow-cone annular jet by passing through the outlet passage. Moreover, the strong shear stress can prevent particles precipitated from adhering in the inner wall of the nozzle. The shear stress at outlet is stronger than before so as to prevent from jam.

The length of swirl chamber (h_2) and the diameter of nozzle outlet (d_0) are the key dimensions for this kind of nozzle. On the one hand, h_2 should satisfy the request of sufficient mixing of solution and SC-CO_2 in order to decrease the solubility of the solute in the solvent to a minimum and to form crystal nuclei after solute precipitating. On the other hand, once precipitating, the solute should be sprayed out immediately so as to reduce the time and the space for crystal nuclei growing. Both of the two aspects require that h_2 should be short as much as possible on condition that solution and SC-CO_2 can mix thoroughly. In regards to d_0, need a suitable value. If the value is too small, the nozzle is prone to be blocked and the turbulence intensity in swirl chamber would be decreased dramatically. However, if the value is too big, the effect of atomization would be reduced greatly and the speed of the mixture in swirl chamber would be decreased. Therefore, it is essential to determinate suitable values of h_2 and d_0 according to the condition of technological process. Whereas, the cost of nozzle manufacture is very high. It will cause great waste if many nozzles are manufactured to test optimal structure values. Moreover, the flow in the nozzle is very complex, involving jet hydrodynamics, mass transfer, phase equilibrium, nucleation and crystal growth kinetics and so forth, which can not be studied only by experiment.

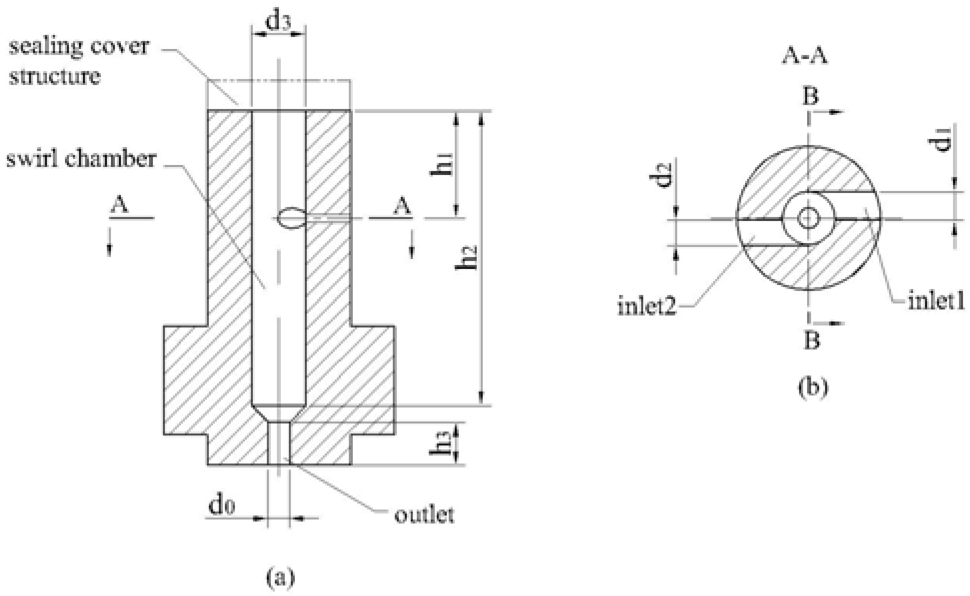

(B-B cross section: the section used in expressing internal flow)

(a) A sectional view of the nozzle. (b) A-A cut of the nozzle

Figure 1. Structure sketch of the tangential-inlet swirl nozzle

However the importance of CFD on the assessment of the efficiency of a SAS precipitation chamber has been clearly demonstrated[12]. Thereby, in this study, CFD was utilized to simulate experiment process and study the mixing and the flow in nozzle in order to optimize the nozzle designed.

NUMERICAL SIMULATION SECTION

Governing Equations

The numerical simulation of the flow in the tangential-inlet swirl nozzle is performed by using a commercial CFD code: Fluent which solves the classical mass, momentum and energy conservation equations to describe the fluid behavior and properties. In this model, primary phase is SCF phase and secondary or dispersed phase is solution phase. The continuity equation for phase *i* is defined as Eq. (1).

$$\frac{\partial}{\partial t}(\alpha_i \rho_i) + \nabla \cdot (\alpha_i \rho_i \vec{u}_l) = \sum_{p=1}^{2} \left(\dot{m}_{pi} - \dot{m}_{ip} \right) \tag{1}$$

where $\vec{u}_l$ is the velocity of phase i and $\dot{m}_{ip}$ characterizes the mass transfer from the *p*th phase to *i*th phase.

The momentum balance for phase *i* yields Eq. (2) [13].

$$\frac{\partial}{\partial t}\left(\alpha_i \rho_i \vec{u}_l\right) + \nabla \cdot \left(\alpha_i \rho_i \vec{u}_l \vec{u}_l\right) = -\alpha_i \nabla P + \nabla \cdot \overline{\tau} + \alpha_i \rho_i \vec{g} + \sum_{p=1}^{2} \left(\vec{R}_{pl} + \dot{m}_{pl} \vec{u}_{pl} - \dot{m}_{pl} \vec{u}_{lp} \right) + \left(\vec{F}_i + \vec{F}_{lift,i} + \vec{F}_{vm,i} \right) \tag{2}$$

where $\overline{\tau}_i$ is the *i*th phase stress strain tensor, $\vec{F}_i$ is an external body force, $\vec{F}_{lift,i}$ is a lift force, $\vec{F}_{vm,i}$ is a virtual mass force, $\vec{R}_{pi}$ is an interaction force between phases and *P* is the pressure shared by all phases. $\vec{u}_{pl}$ is the interphase velocity. If $\dot{m}_{pi} > 0$; $\vec{u}_{pl} = \vec{u}_p$ and if $\dot{m}_{pi} < 0$; $\vec{u}_{pl} = \vec{u}_l$

Computational domain modeling and meshing

The most structure dimensions of the nozzle were designed according to the principle of the process, strength requirements and the dimensions of the co-axial nozzle mentioned in literature [9]. The most structural dimensions are listed in Table 1. The length of swirl chamber h_2 and outlet diameter of the nozzle d_0 were simulated and analyzed in different values so as to determinate the optimal value. The values of h_2 were set respectively to be 4mm, 6mm and 8mm. The values of d_0 were set respectively to be 0.1mm, 0.2mm, 0.3mm, 0.4mm and 0.5mm. According to these dimensions, 3D schematic drawing of computational domain was drawn as shown in Figure 2.

Table 1. The main structural dimensions of the nozzle

geometry parameters	Size (mm)
Diameter of inlet1 d_1	0.4
Diameter of inlet2 d_2	0.35
Diameter of swirl chamber d_3	0.75
Location dimension of inlets h_1	1.5
Length of exit passage h_3	1

After The model of computational domain being established, the next step is to divide it in several cells in which all fluid mechanic equations will be solved. This step is carried out thanks to Gambit 2.4 software. The asymmetry of the nozzle caused by the two inlets forced the model presented herein to be solved in three dimensions in space. The meshing of the nozzle studied by CFD is shown in Figure 3.

Solving methods and numerical method

In SESD process, the flow parameters in nozzle are independent with time, consequently the flow in the nozzle should be regarded as 3D and steady state flow. In order to simulate precipitation in a two-phase system, Eulerian model was selected as Multiphase Model, and the two phases in nozzle were treated as continuum phases. The realizable k–ε turbulence model was selected for turbulent flow calculations. First order upwind discretization schemes were selected to solve volume fraction, momentum, turbulence and energy equations. Pressure-velocity coupling was modeled by using the phase coupled SIMPLE algorithm.

Figure 2 The model of computational domain

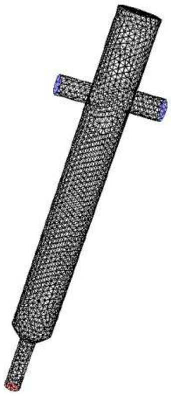

Figure 3 Meshing of the nozzle studied by CFD

Materials and boundary conditions

Solvent and anti-solvent are ethanol and SC-CO_2 respectively [12, 14]. Because the solute contained in the solution is relatively slight, it can be assumed that there are only two fluids in the flow system, and the two fluids are introduced separately from two inlets of nozzle. Another assumption is that the system is considered as incompressible system for CFD simulations[13, 15]. All fluid variations are considered to be isobaric at 10 MPa.

As shown in Fig 1, the inlet1 is the inlet of SC-CO_2 and inlet2 is the inlet of ethanol. A simple mass flow inlet was selected as the inlet boundary condition of inlet. The mass flow and temperature of SC-CO_2 were 5.46×10^{-4}kg/s and 363K respectively. The volume fraction of ethanol was zero. Turbulent kinetic energy *k* can be calculated by equation (4).

$$k = \frac{3}{2}\left(\bar{u}_{ref} I\right)^2 \quad (4)$$

where $\bar{u}_{ref}$ is the mean velocity at inlet, which can be calculated by mass flow rate. *I* is the turbulence intensity of inlet, which can be calculated by Eq. (5).

$$I = 0.16(\mathrm{R}_{eDH})^{-1/8} \quad (5)$$

Turbulent dissipation rate ε is estimated by Eq. (6) and Eq. (7).

$$\varepsilon = 0.09^{3/4}\frac{k^{3/2}}{l} \quad (6)$$

$$l = 0.07L \quad (7)$$

where, *k* is turbulent kinetic energy, *L* is characteristic length, which can be calculated according to the equivalent diameter.

Velocity-inlet was selected as the inlet boundary condition of inlet2. The velocity magnitude of solvent was 0.5m/s. Turbulence intensity was 1% and hydraulic diameter was 0.35mm. The temperature was 313K. Pressure-outlet was selected as boundary condition of outlet. The pressure of outlet was specified as 8Mpa.

RESULTS AND DISCUSSION

It has been confirmed that liquid atomization theory and Weber number based analysis are no longer the appropriate theory and parameter to characterize the SAS process. Instead, gaseous mixing theory and mixing rates, or rather, mixing length scales for turbulent mixing, should be used to characterize sprays of miscible fluids[16]. Therefore in this study, volume fraction of ethanol and turbulence intensity of flow in the nozzle were indicators to test the performance of these nozzles with different dimensions.

Effect of length of swirl chamber

In this series of CFD simulations, the effect of different lengths of swirl chamber on the performance of these nozzles was the main result to be gotten. The diameters of nozzle outlet were all set to be 0.3mm. The length of swirl chamfer was set to be three levels, being respectively 4mm, 6mm and 8mm. Because the change of the flow indicators in the nozzle can not be seen in three-dimensional form, the B-B cross section, as shown in Figure 1, was utilized to observe the change of the flow indicators in the nozzle. Contour of volume fraction of ethanol in different h_2 was shown in Figure 4. Contour of turbulence intensity of mixture in the nozzle in different h_2 was shown in Figure 5.

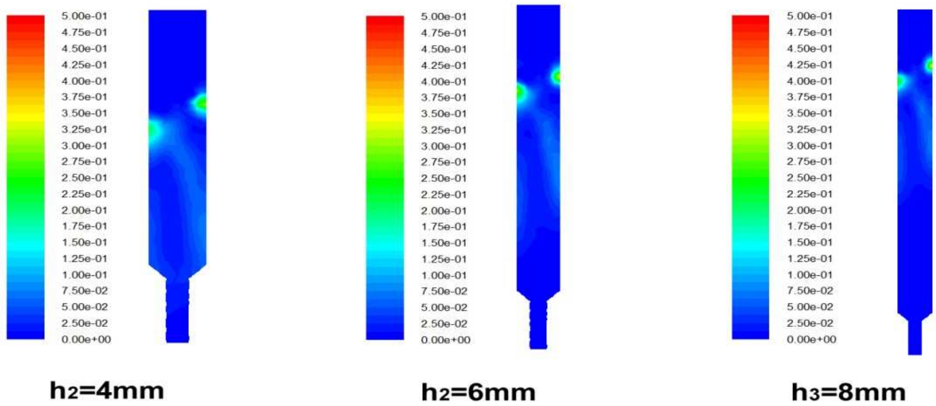

Figure 4. Contour of volume fraction of ethanol in different h_2

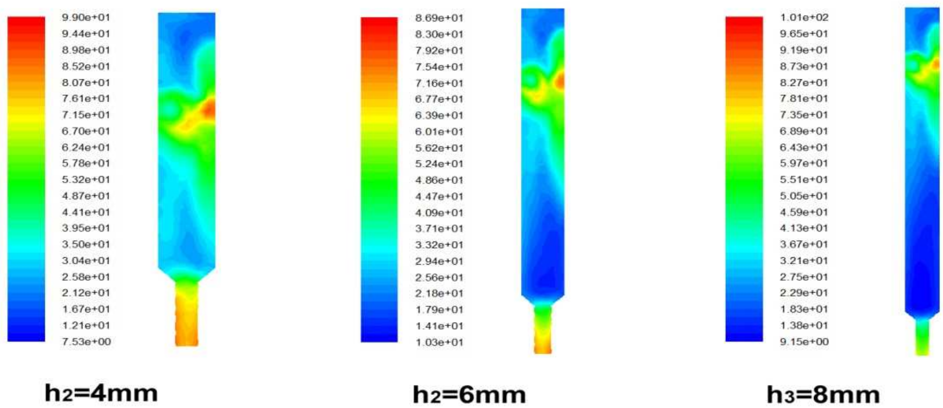

Figure 5. Contour of turbulence intensity of mixture in the nozzle in different h_2

As can be seen from Figure 4, when h_2=4, SC-CO_2 and ethanol did still not mix thoroughly at the lower part of the swirl chamber. In this condition, the anti-solvent effect of SC-CO_2 can not be brought thoroughly into play and there were still some amount of solute dissolved in ethanol, which affected the granulation effects and meant that the length of swirl chamber was not suitable. When h_2=6, volume fraction of ethanol was uniform at the position of near bottom where there was still a short distance for the solute in ethanol to precipitate in anti-solvent effect of SC-CO_2, which accorded the request of preparing nana-drug in SEDS. When h_2=8, SC-CO_2 and ethanol mixed thoroughly at the mid part of the swirl chamber, where is so far from the outlet that the growth time of crystal nuclei precipitate after mixing was too long and the size of particle could not be controlled in nano grade. From Figure 5, one can concluded that with the increase of h_2, the turbulence intensity in lower part increased of the nozzles was relatively low and that in other parts was similar. Overall, Only when h_2=6, the two kind of fluids can mixed thoroughly in the tangential-inlet swirl nozzle, and the nana-particles can be spray out immediately after being precipitated, which decreased the growth time of crystal nuclei and met optimal process requirements.

Effect of diameter of outlet

In this series of CFD simulations, the lengths of swirl chamber were all set to be 6mm. The diameter of outlet was set to be three levels, being respectively 0.1mm, 0.2mm, 0.3mm, 0.4mm and 0.5mm. The simulation results thus obtained are shown in Figure 6 and Figure 7.

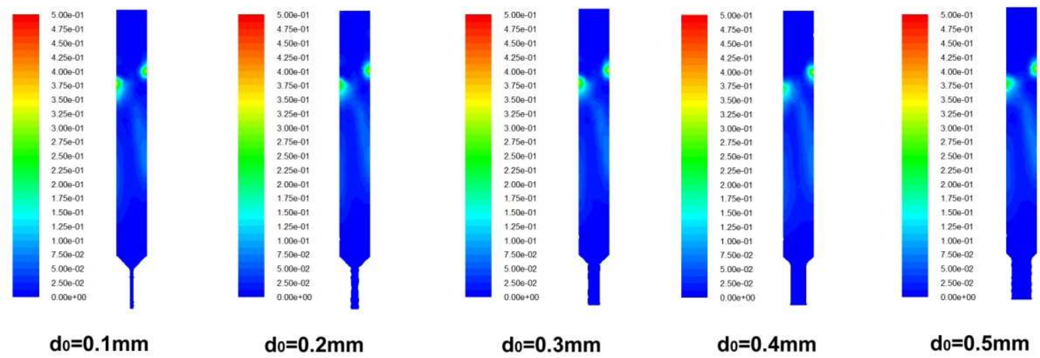

Figure 6. Contour of volume fraction of ethanol in different d_0

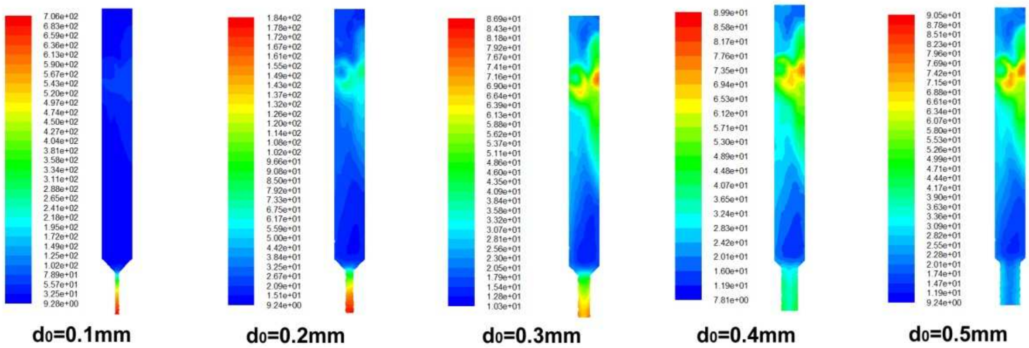

Figure 7. Contour of turbulence intensity of mixture in the nozzle in different d_0

As can be seen from Figure 6, the effect of the value of d_0 on volume fraction of ethanol was little, which meant that mixing degree of SC-CO_2 and ethanol almost not be influenced by the value of d_0. It could be confirmed from Figure 7 that when the value of d_0 is 0.1mm or 0.2mm, on the one hand, because of low turbulence intensity in swirl chamber, the precipitated particles were prone to agglomerate. On the other hand, because of small value of d_0, the outlet tended to be jammed. When d_0 was equal to or greater than 0.3mm, the turbulence intensity in swirl chamber of different nozzles were all meet the requirements of decreasing agglomeration and inhibiting the growth of crystal nuclei. Whereas with the increase of d_0, the turbulence intensity at outlet decreased gradually, which was not conducive to forming small droplet after the mixture being sprayed out and affected the size and size distribution of nano-drug particles. Therefore, when d_0 was 0.3mm, the performance of the tangential-inlet swirl nozzle was optimal.

CONCLUSION

A tangential-inlet swirl nozzle for preparing nano-drug by SEDS process has been designed to optimize gas-like mixing in a micro-mixing volume through the use of swirl. CFD simulation was carried out to analyze and optimize the designed nozzle. Results showed that the tangential-inlet swirl nozzle could achieve full mixing of SC-CO_2 and ethanol, high turbulence intensity, thorough precipitation of solute and relatively short growth time of crystal nuclei. Especially when h_0 was 6mm and d_0 was 0.3mm, the performance of the tangential-inlet swirl nozzle was optimal. By CFD analysis and optimization, the cost of designing suitable nozzle was decreased and the performance of the nozzle was enhanced. The method of CFD analysis used in this work can also be applied to similar systems. This study achieved the using of virtual manufacturing technology in the equipment development of preparing nano-drug in SEDS process.

REFERENCES

[1]H Patel; P Patel; T Brahmbhatt, et al., *J Chem Pharm Res*, **2011**, 3(6), 217-221.
[2]S Sunkara; D Sravanthi; KM Maheswari, et al., *J Chem Pharm Res*, **2013**, 5(1), 320-328.
[3]BN Nalluri; D Jyotheermayi; D Anusha, et al., *J Chem Pharm Res*, **2012**, 4(9), 4266-4274.
[4]E Reverchon; I De Marco; G Della Porta, *J Supercrit Fluids*, **2002**, 23(1), 81-87.
[5]U Anand; J Ambarish, *J Chem Pharm Res*, **2011**, 3(6), 839-845.
[6]BA Domadia; NR Vaghela, *J Chem Pharm Res*, **2013**, 5(4), 188-191.
[7]WZ He; QL Suo; ZH Jiang, et al., *J Supercrit Fluids*, **2004**, 31(1), 101-110.
[8]DJ Jarmer; CS Lengsfeld; TW Randolph, *J Supercrit Fluids*, **2003**, 27(3), 317-336.

[9]J Bałdyga; D Kubicki; BY Shekunov, et al., *Chem Eng Res Des*, **2010**, 88(9), 1131-1141.
[10]Y Chen; S Xiao; H Song, et al., *Journal of Computers*, **2013**, 8(2).
[11]R Yang; Y Zhou; N Zhao, et al., *Journal of Computers*, **2011**, 6(1).
[12]MAT Cardoso; JMS Cabral; AMF Palavra, et al., *J Supercrit Fluids*, **2008**, 47(2), 247-258.
[13]A Leybros; R Piolet; M Ariane, et al., *J Supercrit Fluids*, **2012**, 70, 17-26.
[14]J Bałdyga; R Czarnocki; BY Shekunov, et al., *Chem Eng Res Des*, **2010**, 88(3), 331-341.
[15]S Moussiere; A Roubaud; O Boutin, et al., *J Supercrit Fluids*, **2012**, 65, 25-31.
[16]BY Shekunov; M Hanna; P York, *J Cryst Growth*, **1999**, 198, 1345-1351.